Position Tracking and Path Planning in Uncertain Maps for Robot Formations ⋆

María T. Lázaro, Pablo Urcola, Luis Montano, José A. Castellanos

Instituto de Investigación en Ingeniería de Aragón,
Universidad de Zaragoza, Spain
(e-mail: [mtlazaro, urcola, montano, jacaste]@ unizar.es).

Abstract: This paper presents a complete working system for robot formations, where path planning and localization tasks are integrated in such a way that environment uncertainty is considered in each of the tasks. Feature-based and grid-based mapping strategies are combined in a probabilistic way to compute an obstacle-free and of minimum-risk plan towards the goal. The formation benefits from the cooperative perception to obtain a joint vision of the environment, represented in a leadercentric way to minimize the effects of the uncertainty. The system has been tested and validated by means of a set of simulations as well as in real experiments.

Keywords: Robot formation, planning, localization, risk map, cooperative perception.

1. INTRODUCTION

Robot formations are a specific case of multi-robot system where robots coordinate and cooperate to accomplish a misssion, following a predefined *leader-follower* structure. The wide variety of real applications, such as exploration, surveillance, transport and rescue, require an effort to consistently integrate the information shared by each robot. Many works have been developed related to formations, although most of them work in deterministic and predictable scenarios. However, the need to consider sensor uncertainties and unexpected changes of the environment lead us to propose a whole system that deals with the uncertainties when localization, mapping, global and local planning tasks of the formation are integrated to achieve a mission.

Usually, the formation is provided with a previous map of the environment where it has to carry out the commanded mission, to compute a global path towards the goal. In our case, this map is available to the formation as a feature-based stochastic map which is mapped into a grid map where each cell represents the risk level for traversing a certain area of the environment. While the formation executes the global minimum risk plan towards the goal, unexpected obstacles not considered in the previous map may appear. A local planner computes then a local risk-based path by using the uncertain sensorial information shared by the robots. It is executed by the formation motion control by using a spring-damper analogy to drive the robots, which adapt the formation structure to the shape and dynamism of the environment. During the execution of the path, the localization system minimizes the robots uncertainty location using the new information captured and the previous stochastic map.

⋆ This work was partially supported by the Spanish projects MICINN-FEDER DPI2009-08126 and DPI2009-13710, and the European project UE-ICT-2009-248942.

The problem of planning under uncertainty is treated in different ways in the literature. Some works take into account the uncertainty of the environment, like Missiuro and Roy (2006) who search the trajectory that minimizes the expected cost of collision by using probabilistic roadmaps under the assumption of independence in the probability distribution of the obstacles. Nakhaei and Lamiraux (2008) propose a framework about planning motions for humanoid robots in changing environments using occupancy-grids based maps where the cells are labeled as occupied, unknown or free. Other kind of works focus on the uncertainty of the path, like Censi et al. (2008) who seek the path which minimizes the uncertainty at the goal, leading to paths that are no optimal in terms of Euclidean distance to the goal. Berg et al. (2010) try to obtain prior probability distributions of the states and the control inputs of the robot for a previously computed path taking into account the motion and sensing uncertainties. These techniques lead to local variations from the path that may not be able to deal with big deviations needed in some scenarios.

Regarding formation control, many papers have been published using leader-followers approaches like in Gustavi and Hu (2008); Loizou and Kyriakopoulos (2008). In Urcola and Montano (2009) we developed cooperative formation motion planning techniques that allows adapting the formation configuration to changes of the environment. In this work we extend those techniques focusing on the aspects of cooperatively building a common uncertain map of the environment from all the robots of the team for localization and planning.

Regarding to multi-robot localization, some works like Roumeliotis and Bekey (2002) make use of inter-robot measurements to localize a team of robots. When an *a priori* map is available to the team, the localization process depends on the kind of map used, usually features or grids (Schultz and Adams (1998)). The use of feature-based stochastic maps to localize a robot formation was

addressed in Lázaro and Castellanos (2010) where inconsistency problems due to the existence of time-correlated measurement sequences were reported and the use of the Measurement Differencing technique was proposed to efficiently improve consistency. In this paper, we propose an extension of that localization algorithm (MD-EKF) to also improve the observations gathered by the robots and to obtain a more coherent vision of the environment.

This paper is organized as follows: section 2 defines the probabilistic model of the robot formation localization with its uncertainty. In section 3 the motion planning techniques are presented in the framework of the probabilistic model. In section 4, simulations and a real experiment are reported. Finally, we conclude in section 5.

2. PROBABILISTIC ROBOT FORMATIONS

Let a robot formation be composed of $r+1$ heterogeneous vehicles $\{R_0, R_1, ..., R_r\}$, where R_0 is the robot leader and $R_j, j = \{1, ..., r\}$ are the robot followers. A certain geometric shape, e.g. equilateral triangle, regular pentagon, etc, is imposed to the team depending on the number of vehicles and the task commanded to the formation.

From a probabilistic geometrical view-point, the location of the robot formation can be represented by a discrete-time stochastic state vector $\mathbf{x}_\mathcal{R}$ formed by the location of the robot leader R_0 with respect to (wrt) a base reference frame B and the location of each robot follower R_j wrt the robot leader R_0, and by its associated covariance matrix $\mathbf{P}_\mathcal{R}$, which stores the statistical dependencies between those estimated locations. Following the Gaussinity assumption, $\mathbf{x}_\mathcal{R} \sim \mathcal{N}(\hat{\mathbf{x}}_\mathcal{R}, \mathbf{P}_\mathcal{R})$ with,

$$\hat{\mathbf{x}}_\mathcal{R} = \begin{pmatrix} \hat{\mathbf{x}}^B_{R_0} \\ \hat{\mathbf{x}}^{R_0}_{R_1} \\ \vdots \\ \hat{\mathbf{x}}^{R_0}_{R_r} \end{pmatrix}; \mathbf{P}_\mathcal{R} = \begin{pmatrix} \mathbf{P}_{R_0} & \cdots & \mathbf{P}_{R_0 R_r} \\ & \ddots & \\ \mathbf{P}_{R_r R_0} & \cdots & \mathbf{P}_{R_r} \end{pmatrix} \quad (1)$$

This leader-centric representation reduces the volume of uncertainty, i.e. the determinant of the covariance matrix $\mathbf{P}_\mathcal{R}$, in comparison with an absolute representation wrt the base frame B of each robot location vector and, therefore, linearization errors due to large uncertainty values are minimized (Castellanos et al. (2007)).

2.1 Pose Tracking of the Robot Formation

Using the dynamical model of the robot formation based on a virtual spring-damper analogy (Urcola and Montano (2009), figure 1) the state of the robot formation is propagated from time step $k-1$ to time step k using the motion model

$$\mathbf{x}_{\mathcal{R}_k} \simeq \mathbf{F}_{k-1}\mathbf{x}_{\mathcal{R}_{k-1}} + \mathbf{v}_{k-1} \quad (2)$$

where the block-diagonal matrix $\mathbf{F}_{k-1}$ represents the Jacobian matrix of the linearized motion equations of the robot team and $\mathbf{v}_{k-1}$ represents a zero-mean white noise sequence with a block-diagonal covariance matrix $\mathbf{Q}_{k-1}$.

Let $\mathbf{x}_k$ be an augmented state vector defined as,

$$\mathbf{x}_k = \begin{pmatrix} \mathbf{x}_{\mathcal{R}_k} \\ \mathbf{y}_{\mathcal{E}_k} \end{pmatrix} \quad (3)$$

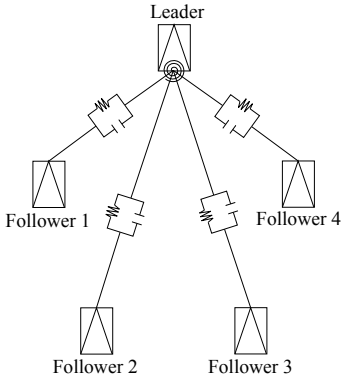

Fig. 1. Spring-damper analogy for a pentagon-shaped robot formation. Linear and torsional springs and dampers are combinded to induce virtual forces between the linked robots.

where $\mathbf{x}_{\mathcal{R}_k}$ is the discrete-time stochastic state vector of the robot formation localization and $\mathbf{y}_{\mathcal{E}_k}$ relates to the relative localization vector of the gathered observations. Also, let $\mathbf{P}_k = \text{blkdiag}(\mathbf{P}_{\mathcal{R}_k}, \mathbf{P}_{\mathcal{E}_k})$ be its joint covariance matrix.

At time step k, cooperative perception of the environment by the team of heterogeneous robots together with robust data association techniques, provide a set of jointly consistent pairings $(\mathbf{y}_{\mathcal{E}_k}, \mathbf{y}_{\mathcal{F}_k})$ between the current sensor observations $\mathbf{y}_{\mathcal{E}_k}$ and map features $\mathbf{y}_{\mathcal{F}_k}$ derived from an a priori known stochastic map of the environment, $\mathcal{M}^B_\mathcal{F} = \{\hat{\mathbf{y}}^B_\mathcal{M}, \mathbf{P}^B_\mathcal{M}\}$, where $\hat{\mathbf{y}}^B_\mathcal{M} = \{\hat{\mathbf{y}}^B_{F_1}, \hat{\mathbf{y}}^B_{F_2}, ..., \hat{\mathbf{y}}^B_{F_n}\}$ is a vector containing the estimated location of the map features $\mathcal{F} = \{F_1, F_2, ..., F_n\}$ wrt to a base reference frame B and $\mathbf{P}^B_\mathcal{M}$ its associated covariance matrix, all related by a measurement equation of the form of

$$\mathbf{f}_k(\mathbf{x}_\mathcal{R}, \mathbf{y}^B_\mathcal{M}, \mathbf{y}_\mathcal{E}) = \mathbf{0} \quad (4)$$

Due to the inherent nonlinearities, a linearized measurement equation is used within the EKF-update step:

$$\mathbf{z}_k \simeq \mathbf{H}_k\mathbf{x}_k + \mathbf{G}_{\mathcal{F}_k}\mathbf{y}_{\mathcal{F}_k} \quad (5)$$

where $\mathbf{H}_k = (\mathbf{H}_{\mathcal{R}_k} \ \mathbf{H}_{\mathcal{E}_k})$ and $\mathbf{G}_{\mathcal{F}_k}$ are the Jacobian matrices of the linearized measurement equations with respect to the state vector $\mathbf{x}_k$ and the matched features $\mathbf{y}_{\mathcal{F}_k}$ respectively.

Colored Measurement Equation As reported in Lázaro and Castellanos (2010), the use of subsets of map features $\mathcal{F}_{k-1}$ and $\mathcal{F}_k$ in consecutive time steps related within the stochastic map by a cross-correlation term $\mathbf{P}_{\mathcal{F}_{k-1}\mathcal{F}_k}$ makes necessary the consideration of a colored measurement noise scheme, otherwise, the estimation would lead to inconsistency. Following the seminal work of Bryson and Johansen (1968) and recent practical approaches Petovello et al. (2009) and Lázaro and Castellanos (2010), a measurement differencing technique is considered to efficiently remove the time-correlated portion of the measurement errors.

The nature of the colored noise driving eq. (5) could be modeled by the linear transformation relating the two matched map features at time instants $k-1$ and k formulated as,

$$\mathbf{y}_{\mathcal{F}_k} = \mathbf{F}_{C_k}\mathbf{y}_{\mathcal{F}_{k-1}} + \mathbf{n}_k \quad (6)$$

where,

$$\mathbf{F}_{C_k} = \mathbf{P}_{\mathcal{F}_k\mathcal{F}_{k-1}}\mathbf{P}^{-1}_{\mathcal{F}_{k-1}} \quad (7)$$

and $\mathbf{n}_k$ is assumed to be a zero-mean white noise measurement sequence with covariance matrix,

$$\mathbf{P}_{\mathbf{n}_k} = \mathbf{P}_{\mathcal{F}_k} - \mathbf{P}_{\mathcal{F}_k\mathcal{F}_{k-1}}\mathbf{P}^{-1}_{\mathcal{F}_{k-1}}\mathbf{P}_{\mathcal{F}_{k-1}\mathcal{F}_k} \tag{8}$$

Whitened Measurement Equation The measurement differencing technique provides a whitened measurement equation from the weighted difference of colored measurement equations (of the form of eq. 5) at two consecutive time instants,

$$\mathbf{r}_k \triangleq \mathbf{z}_k - \mathbf{\Lambda}_k\mathbf{z}_{k-1} \tag{9}$$

where matrix $\mathbf{\Lambda}_k$ is chosen such that the discrete-time stochastic process $\{\mathbf{r}_k, 0 \leq k < \infty\}$ is driven by white-noise only.

Following a similar derivation given in Lázaro and Castellanos (2010), eq. (9) can be rewritten as,

$$\mathbf{r}_k \simeq \mathbf{H}^*_k\mathbf{x}_k + \mathbf{w}_k \tag{10}$$

where

$$\mathbf{H}^*_k \simeq \left(\mathbf{H}_{\mathcal{R}_k} - \mathbf{\Lambda}_k\mathbf{H}_{\mathcal{R}_{k-1}}\mathbf{F}^{-1}_{k-1} \;\; \mathbf{H}_{\mathcal{E}_k} \right) \tag{11}$$

and the white noise sequence $\mathbf{w}_k$, with covariance matrix $\mathbf{P}_{\mathbf{w}_k}$, is given by,

$$\mathbf{w}_k \simeq \mathbf{\Lambda}_k\mathbf{H}_{\mathcal{R}_{k-1}}\mathbf{F}^{-1}_{k-1}\mathbf{v}_{k-1} + \mathbf{G}_{\mathcal{F}_k}\mathbf{n}_k \tag{12}$$

and,

$$\mathbf{\Lambda}_k \simeq \mathbf{G}_k\mathbf{F}_{C_k}\mathbf{G}^T_{\mathcal{F}_{k-1}}(\mathbf{G}_{\mathcal{F}_{k-1}}\mathbf{G}^T_{\mathcal{F}_{k-1}})^{-1} \tag{13}$$

Finally, the classical EKF update equations provide estimates for the state vector $\mathbf{x}_k$ and its associated covariance matrix $\mathbf{P}_k$ using the filter gain given by,

$$\begin{aligned}\mathbf{K}_k = &(\mathbf{P}_{k|k-1}\mathbf{H}^{*T}_k + \mathbf{C}_k) \cdot \\ &(\mathbf{H}^*_k\mathbf{P}_{k|k-1}\mathbf{H}^{*T}_k + \mathbf{P}_{\mathbf{w}_k} + \mathbf{H}^*_k\mathbf{C}_k + \mathbf{C}^T_k\mathbf{H}^{*T}_k)^{-1}\end{aligned} \tag{14}$$

with,

$$\mathbf{P}_{k|k-1} = \text{blkdiag}\left(\mathbf{F}_{k-1}\mathbf{P}_{\mathcal{R}_{k-1}}\mathbf{F}^T_{k-1} + \mathbf{Q}_{k-1}, \mathbf{P}_{\mathcal{E}_k}\right)$$

and $\mathbf{C}_k$, the correlation term between $\mathbf{v}_{k-1}$ and $\mathbf{w}_k$ derived from eq (12),

$$\mathbf{C}_k = E[\mathbf{v}_{k-1}\mathbf{w}^T_k] = \mathbf{Q}_{k-1}(\mathbf{\Lambda}_k\mathbf{H}_{\mathcal{R}_{k-1}}\mathbf{F}^{-1}_{k-1})^T$$

3. PATH PLANNING UNDER UNCERTAINTY

Path planning task has been divided in two different levels: A global plan that computes a safe path from the starting point to the goal based on a previously computed risk map and a local plan that incorporates the information gathered from the sensors during the execution. Both path planners use risk maps to model the environment where the formation is moving.

3.1 Risk Maps

A risk map could be defined as the probabilistic projection of the feature-based stochastic map into a grid-based representation of the environment. The risk level of a cell represents the probability of the presence features in the cell and, as a consequence, the probability of being a non-traversable cell.

Computing for each cell in the grid the exact risk level is too expensive in time to accomplish it during the execution of the mission. That is the reason why we have adopted an approximate solution that consists in sampling the probability distribution of the features in the map. The samples are then represented into the grid and the number of samples that are projected at each cell is used as an approximation of the risk level, after a normalization process.

3.2 Global minimum risk paths

Using the a priori stochastic map of the environment $\mathcal{M}^B_{\mathcal{F}}$, a traversable path could be computed using the A* algorithm adapted for risk maps. The optimal path, computed at the beginning of the mission, will be the one that minimizes the risk, so that the robots are more likely to reach their goal safely.

In order to minimize the risk of the global path, we threshold the risk map obtained from the a priori map of the environment. Cells are labeled as traversable if their risk level is lower than the threshold and non-traversable otherwise. A* algorithm is used to find the shortest path to the goal using only traversable cells. If the goal is not reachable at a certain risk level, the threshold is increased, and thus the risk level, and the A* algorithm is used again. At the end, π the path with the minimum risk level required to reach the goal is obtained. Note that this computation is preformed before the navigation starts using only the a priori map of the environment.

3.3 Local minimum risk paths

Using the global path π, the formation obtain a list of waypoints to navigate through in order to reach the final goal. However, in dynamic environments, the global path may become unfeasible because of new obstacles not present in the previous map. Also, the risk of traversing some zones in the environment may have changed.

The local planner computes the optimal path, in terms of distance and risk, to the next waypoint in the global path that may be reached. Only the leader of the formation computes the local path using the information $\mathbf{y}_{\mathcal{E}_k}$ gathered from the sensors of all the robots. Using a common local map for all the formation improves the perception of the environment by augmenting the individual views. Moreover, in order to reduce the uncertainty due to the global localization of the robots, and thus the risk, a robocentric grid map is adopted for the local path planning. However, as we are considering a multi-robot system, the uncertainty of the relative localization of the robots is taken into account.

Instead of thresholding the risk map to define the traversability of the cells, as proposed in the global path planning, we define in equation (16) a traversability cost function that increases with the risk. The path planning algorithm finds the path to the next waypoint that minimizes the total cost (15). We have adopted this approach for local path planning to smooth the changes that may happen in the environment.

$$\text{totalcost} = \sum_{k=1}^{goal} dist((c^{k-1}_{ij}, c^k_{ij})cost(c^k_{ij}) \tag{15}$$

$$cost(c_{ij}) = \begin{cases} \infty, & \text{if } (i,j) \in \mathbf{y}_{\mathcal{E}_k} \\ 1/(1 - risk(i,j)), & \text{otherwise} \end{cases} \quad (16)$$

The local map is updated as the sensors gather newer information from the environment. The changes in the map are only considered if they are in the field of view of the formation. Due to the uncertainty in the measurements and in the relative localization of the robots, the field of view is also considered in a probabilistic manner. Using an analogue algorithm as the one used to compute the risk maps, we compute for each cell the probability of being perceived by the formation and, as a consequence, only those cells that have a high probability of being observed are considered for updating the local map.

To conclude, Figure 2 shows an schema of the relationships among the components of the system presented above and the pseudo-code for the leader and the followers are presented in Algorithms 1 and 2.

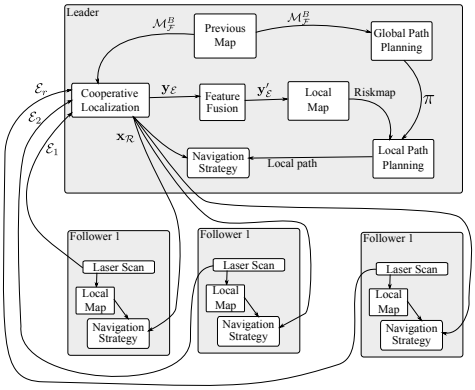

Fig. 2. System overview including the components, their relationships, the data they interchange and where they are executed.

Algorithm 1 Leader algorithm

{Algorithm for the Leader}
Require: $\mathbf{x}_{start}, \mathbf{x}_{goal}, \mathcal{M}^B_{\mathcal{F}}$
$\pi \leftarrow computeGlobalPath(\mathbf{x}_{start}, \mathbf{x}_{goal}, \mathcal{M}^B_{\mathcal{F}})$
while last waypoint of π not reached **do**
$\mathcal{E} \leftarrow gatherObservationsFromRobots()$
$\langle \mathbf{x}_{\mathcal{R}}, \mathbf{y}_{\mathcal{E}} \rangle \leftarrow MD - EKF(\mathcal{E})$
$\mathbf{y}_{\mathcal{E}} \leftarrow fuseFeatures(\mathbf{y}_{\mathcal{E}})$
$R \leftarrow buildLocalRiskmap(\mathbf{y}_{\mathcal{E}})$
$sendInfoToFollowers(\mathbf{x}_{\mathcal{R}})$
$\pi_{local} \leftarrow computeLocalPath(R, \pi)$
$S_{leader} \leftarrow LeaderNavigationStrategy(\mathbf{x}_{\mathcal{R}}, \pi_{local})$
$moveLeader(S_{leader})$
end while

Algorithm 2 Followers algorithm

{Algorithm for Follower i}
while leader keeps moving **do**
$\mathcal{E}_i \leftarrow gatherObservationsFromSensors()$
$sendObservationsToLeader(\mathcal{E}_i)$
$\mathbf{x}_{\mathcal{R}} \leftarrow getInfoFromLeader()$
$S_{follower_i} \leftarrow decideFollowerStrategy(\mathbf{x}_{\mathcal{R}}, \mathcal{E}_i)$
$moveFollower(S_{follower_i})$
end while

4. EXPERIMENTAL RESULTS

Throughout this section, we want to illustrate the benefits of the integration scheme developed in this paper. In the simulation experiments, we describe the computation of global and local minimum risk plans and show the benefits of cooperative perception in re-planning tasks. Then, in a real setting, the integration scheme would be analyzed in a hybrid, centralized-decentralized, architecture with wireless communication capabilities where real-time constraints are a fundamental issue.

4.1 Global and Local Minimum Risk Plans

Figure 3a displays a previously built stochastic map (note sharp edges at the top left part of the figure and blurred edges at the bottom right due to the higher distance to the base reference frame) of an office-like environment. Two possible global paths connect the initial location of the robot formation (labeled as *Start*) and its commanded final destination (labeled as *Goal*): (i) a path through a long curved corridor, or (ii) a path traversing a door (labeled in the figure) unobservable from the initial location.

Figures 3c and 3d show the sensitivity of the algorithm that dramatically changes the path planned for two diferents risk levels (0.1 and 0.05 respectively). By setting the risk level to 0.1 the path planner selects a shorter but more risky path (figure 3c) traversing the door, unobservable from the initial location and with a significant location uncertainty computed during the prior mapping stage. Conversely, setting the risk level to 0.05 results in a more conservative strategy, that avoids traversing the uncertain door, with a longer but safer path (figure 3d) to the goal destination.

Planning a risky path from a global perspective (figure 3e red line traversing the uncertain door) may lead to replanning during the execution, and therefore longer than expected paths to the goal destination, suggested by the local planner due to the observations gathered by on-board sensors: Once the leader of the formation has reached the top right entrance of figure 3f (a zoomed view of figure 3e) the suggested path turns into a dead-end forcing replanning to be conducted.

Finally, it is worth mentioning that, given two different stochastic maps (figures 3a and 3b) a closely related risk map (figure 3d) could be computed from the correct selection of risk levels. Therefore, in a real setting, it would be difficult to differentiate between highly uncertain open spaces and close spaces.

4.2 Feature fusion and replanning

The aim of the next simulation is to show the fusion of the robots' maps into a unique map managed by the leader, and a local replanning derived from the new fused map.

In the scenario depicted in figure 4(e), the formation is navigating towards the goal, and, suddenly, a change appears in the environment when a door is opened. This change is out of the field of view of the leader and thus is not represented in its individual view in figure 4(a). The followers, however, perceive the change in the environment

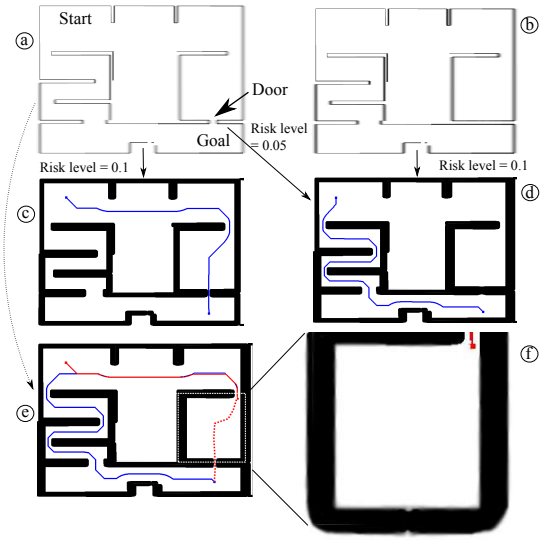

Fig. 3. Influence of uncertainty in global planning

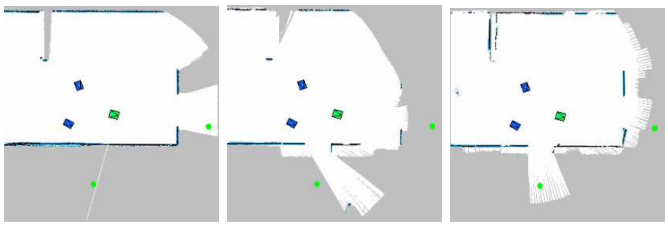

(a) Leader view (b) Follower 1 view (c) Follower 2 view

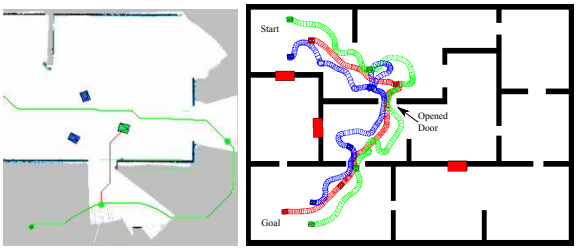

(d) Fused view with the local and the global path (e) Trajectory of the formation

Fig. 4. The small images are the individual views of the robots in the formation. Figure 4(d) shows the result of fusing the view of all the robots and how the leader (in green) takes advantage to compute a new local path (in red) to a different waypoint of the global path (in green).

(see figures 4(b) and 4(c)) and transmit their observations through the network. So the fused map is updated, as shown in figure 4(d)). In this situation, the local planner finds a path to another waypoint of the global plan that is shorter than going to the next waypoint.

Concerning the performance of the localization algorithm, we have measured the consistency and error (figure 5) of the robot formation localization along the trajectory the experiment. It can be seen that the estimations remain consistent along all the simulation (figure 5(a)). Figure 5(b) depicts the error obtained in each component of the position estimation for one robot which is bounded by the limits of the covariance.

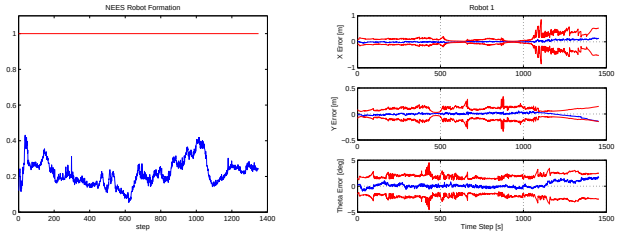

(a) (b)

Fig. 5. Consistency ratio of the robot formation (5(a)) and errors (5(b))in the position (x, y) and orientation (theta) of one of the robots. 2σ uncertainty bounds are depicted in red.

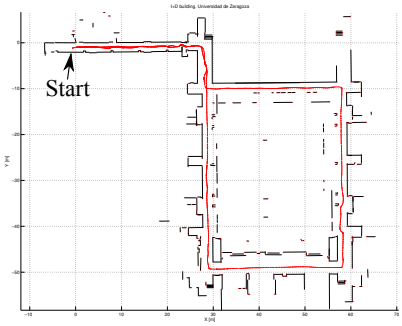

(a)

(b) (c)

(d) (e)

Fig. 6. Real scenario where the experiments have taken place. The trajectory of the formation (a) and other captures during the experiment are shown.

4.3 Experiments in a real scenario

A formation of two Pioneer 3-AT robots equipped with SICK LMS-200 laser rangefinders and, in the case of the follower, also with a Hokuyo URG-04LX laser, is commanded to navigate around a 250 m loop trajectory inside the building shown in figure 6. A segment-based stochastic map of the environment (fig. 6(a)) is available by the formation which is used to compute the global path to reach the goal.

During the experiment, the widest zone of the building, shown in figure 6(b), is also the most populated. The presence of people required the robots to avoid them,

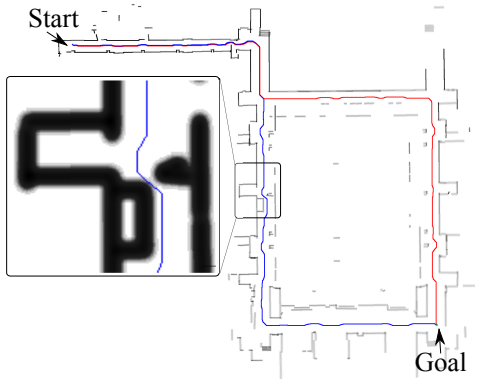

Fig. 7. Two different path are obtained in a slightly changed scenario. The zoom shows a representation of the traversability depending on the risk level considered.

which prevents the robots from recovering the predefined initial configuration, showing the adaptability to static and moving objects in the scenario.

Figure 7, shows the probabilistic projection of the a priori feature-based stochastic map into a risk map. It can be observed a higher uncertainty in the farthest areas from the initial location (top left). The shortest global path planned in this map and the executed one, the same, are shown in figure 6(a). But if a small change is produced in the scenario, for example a box like the one in picture 6(d) is placed in the corridor, the global plan changes, as shown in figure 7. The uncertainty of the box is big in relation with the space for avoiding it when navigating along the corridor and thus the risk of traversing this stretch is higher. This leads to differences between the shortest path and the safest one, because, depending on the risk level, the corridor is considered traversable or not.

Regarding implementation, a high synchronization level is necessary because the leader would need the observations from the follower before computing the localization. Communications among robots have been carried out over a real time wireless multi-hop protocol Tardioli and Villarroel (2007). On the one hand, the team localization and path planning are implemented on the integrated map in a centralized way in the leader. On the other hand, the navigation of the robots is a decentralized process, in which each robot plans and navigates using its own map but using the robot localizations improved by the leader centralized process. Among all these tasks, path planning, executed in the leader, requires most of the computational cost. Anyway, most of the time, the total computational cost per execution cycle is bounded by the 250ms SICK laser refresh time.

5. CONCLUSION

This paper contributes in the field of multi-robot systems, integrating the different techniques involved in such a kind of systems: cooperative perception, mapping and planning, managing several sources of uncertainty through a stochastic model which is jointly exploited by all the mentioned techniques in the same stochastic framework.

Still there are several open issues. The improved uncertain localization of the leader, transmitted to the followers could be reduced if the robots detect and identify each other, and so the relative localization would reduce the global uncertainty of the formation. In some maneuvers, mainly when a replanning is achieved, the automatic change of the role for leader and followers would avoid enforced movements for the followers, detected in the experiments. A more distributed scheme would permit the extension of these techniques to multi-robot systems not in formation.

REFERENCES

Berg, J.V.D., Abbeel, P., and Goldberg, K. (2010). LQG-MP: Optimized path planning for robots with motion uncertainty and imperfect state information. In *Proc. of Robotics: Science and Systems*. Zaragoza, Spain.

Bryson, A.E. and Johansen, D.E. (1968). Linear filtering for time-varying systems using measurements containing colored noise. *IEEE Trans. on Automatic Control*.

Castellanos, J.A., Martinez-Cantin, R., Tardós, J.D., and Neira, J. (2007). Robocentric map joining: Improving the consistency of EKF-SLAM. *Robotics and Autonomous Systems*, 55(1), 21–29.

Censi, A., Calisi, D., Luca, A.D., and Oriolo, G. (2008). A bayesian framework for optimal motion planning with uncertainty. In *Proc. of the IEEE Int. Conf. on Robotics and Automation*, 1798–1805. Pasadena, CA, USA.

Gustavi, T. and Hu, X. (2008). Observer-Based Leader-Following Formation Control Using Onboard Sensor Information. *IEEE Transactions on Robotics*, 24(6), 1457–1462.

Lázaro, M.T. and Castellanos, J.A. (2010). Localization of probabilistic robot formations in SLAM. In *Proc. of the IEEE Int. Conf. on Robotics and Automation*, 3179–3184. Anchorage, Alaska.

Loizou, S. and Kyriakopoulos, K. (2008). Navigation of multiple kinematically constrained robots. *IEEE Transactions on Robotics*, 24(1), 221–231.

Missiuro, P.E. and Roy, N. (2006). Adapting probabilistic roadmaps to handle uncertain maps. In *Proc. of the IEEE Int. Conf. on Robotics and Automation*, 1261–1267.

Nakhaei, A. and Lamiraux, F. (2008). Motion planning for humanoid robots in environments modeled by vision. In *IEEE-RAS International Conference on Humanoid Robots*, 197–204.

Petovello, M.G., O'Keefe, K., Lachapelle, G., and Cannon, M.E. (2009). Consideration of time-correlated errors in a Kalman filter applicable to GNSS. *Journal of Geodesy*, 83, 51–56.

Roumeliotis, S.I. and Bekey, G.A. (2002). Distributed multi-robot localization. *IEEE Trans. on Robotics and Automation*, 18(5), 781–795.

Schultz, A.C. and Adams, W. (1998). Continuous localization using evidence grids. In *Proc. of the IEEE Int. Conf. on Robotics and Automation*. Leuven, Belgium.

Tardioli, D. and Villarroel, J.L. (2007). Real time communications over 802.11: RT-WMP. In *Proc. IEEE International Conference on Mobile Adhoc and Sensor Systems MASS*, 1–11. Pisa, Italy.

Urcola, P. and Montano, L. (2009). Cooperative robot team navigation strategies based on an environmental model. In *Proc. of the IEEE/RSJ Int. Conf. on Intelligent Robots and Systems*. St. Louis, MO.